

# Flipping of antiferromagnetic to superconducting states in pressurized quasi-one-dimensional manganese-based compounds

Sijin Long,<sup>1,2,\*</sup> Long Chen<sup>1,2,\*</sup>, Yuxin Wang,<sup>1,2,\*</sup> Ying Zhou,<sup>1,2,\*</sup> Shu Cai,<sup>1</sup> Jing Guo<sup>1,4</sup>, Yazhou Zhou,<sup>1</sup> Ke Yang,<sup>3</sup> Sheng Jiang,<sup>3</sup> Qi Wu,<sup>1</sup> Gang Wang<sup>1,2,4,†</sup>, Jiangping Hu,<sup>1,2,‡</sup> and Liling Sun<sup>1,2,4,§</sup>

<sup>1</sup>Beijing National Laboratory for Condensed Matter Physics, Institute of Physics, Chinese Academy of Sciences, Beijing 100190, China

<sup>2</sup>University of Chinese Academy of Sciences, Beijing 100049, China

<sup>3</sup>Shanghai Synchrotron Radiation Facilities, Shanghai Institute of Applied Physics, Chinese Academy of Sciences, Shanghai 201204, China

<sup>4</sup>Songshan Lake Materials Laboratory, Dongguan, Guangdong 523808, China



(Received 30 July 2022; revised 26 November 2022; accepted 6 December 2022; published 16 December 2022)

One of the universal features of unconventional superconductors is that the superconducting (SC) state is developed in the proximity of an antiferromagnetic (AFM) state. Unified understanding the interplay between these two states in different superconducting systems is one of the key issues to uncover the underlying physics of unconventional SC mechanism. Here, we report a pressure-induced superconductivity in the quasi-one-dimensional CsMn<sub>6</sub>Bi<sub>5</sub> compound that bears an AFM state at ambient pressure. The SC state appears at the critical pressure ( $P_c$ ) of  $\sim 12$  GPa and stabilizes up to  $\sim 27$  GPa. The high-pressure x-ray-diffraction measurements on CsMn<sub>6</sub>Bi<sub>5</sub> indicate that no structural phase transition occurs at the  $P_c$ , indicating that the AFM-SC transition is electronic in origin. By comparing the previous results of AMn<sub>6</sub>Bi<sub>5</sub> ( $A = \text{K, Rb}$ ), we identify that all members of the family possess the genetic flipping behavior of AFM-SC states at almost the same  $P_c$ , though their ambient-pressure unit-cell volumes vary quite differently. Our theoretical calculations suggest that the pressure-induced changes of partial density of state contributed by the  $d_{yz}$  and  $d_{xz}/d_{z^2}$  orbital electrons near Fermi energy may be associated with the origin of the flipping. These results provide a diverse picture of the connection between the AFM and SC states in the  $3d$ -transition-metal compounds.

DOI: [10.1103/PhysRevB.106.214515](https://doi.org/10.1103/PhysRevB.106.214515)

## I. INTRODUCTION

The  $3d$ -transition-metal compounds with various magnetic ordered states can often be tuned into an unconventional superconductor by adopting nonthermal control parameters, such as chemical doping, external pressure, and magnetic field. Notable examples include cuprates [1,2], iron pnictides [3,4], Cr-based compounds [5], Ni-based compounds [6], and Mn-based binary compounds [7,8], in which the superconductivity develops in the proximity of the magnetic ordered state. How to understand the interplay between the magnetic state and the superconducting (SC) state has been a long-standing challenge for the fields of condensed-matter physics and materials sciences [9–16]. Recently, a new class of ternary compounds, AMn<sub>6</sub>Bi<sub>5</sub> ( $A = \text{Na, K, and Rb}$ ) with a quasi-one-dimensional (Q1D) characteristic, has been found. Structurally, these compounds possess a monoclinic structure with the unique [Mn<sub>6</sub>Bi<sub>5</sub>]-A-[Mn<sub>6</sub>Bi<sub>5</sub>] aligning along the  $b$  axis [17–19]. In particular, the presence of the AFM long-range ordered state in their ambient-pressure phase makes this family greatly attractive. Application of external pressure on the KMn<sub>6</sub>Bi<sub>5</sub> and RbMn<sub>6</sub>Bi<sub>5</sub> compounds finds that the AFM

state is suppressed and then a SC transition is seen [20,21], which provides a platform for investigating the correlation between the AFM and SC states. Here, we take the CsMn<sub>6</sub>Bi<sub>5</sub> compound, a member of this family, as the target material to investigate the pressure-induced superconductivity in this compound, then find a generic behavior existing in the family of AMn<sub>6</sub>Bi<sub>5</sub> ( $A = \text{K, Rb and Cs}$ ), and finally acquire fresh information for better understanding of the underlying mechanism of unconventional superconductors.

## II. RESULTS AND DISCUSSION

CsMn<sub>6</sub>Bi<sub>5</sub> shares the same Q1D structure motif as AMn<sub>6</sub>Bi<sub>5</sub> ( $A = \text{Na, K, and Rb}$ ), as shown in Fig. 1(a). It crystallizes in a monoclinic space group  $C2/m$  (No. 12) with  $a = 23.6338(14)$  Å,  $b = 4.6189(3)$  Å,  $c = 13.8948(8)$  Å, and  $\beta = 125.4468^\circ(20)$  [19]. When the electric current is applied either perpendicular or parallel to the  $b$  axis, the plot of resistance versus temperature of the sample displays the feature of an AFM transition at  $T_N = 81$  K, and exhibits a larger anisotropic resistivity ratio ( $r_{2K} = \rho_{\perp}/\rho_{\parallel} \sim 50$ ) at lower temperature [Fig. 1(b)]. The magnetic susceptibility and heat-capacity measurements further confirm that the AFM transition occurs at  $\sim 81$  K in our ambient-pressure sample [Figs. 1(c) and 1(d)].

First, we performed *in situ* resistance measurements on the CsMn<sub>6</sub>Bi<sub>5</sub> sample in the pressure range of 2.7–11.6 GPa by using a diamond-anvil cell [Fig. 2(a)]. The details about the

\*These authors contributed equally to this work.

†gangwang@iphy.ac.cn

‡jphu@iphy.ac.cn

§llsun@iphy.ac.cn

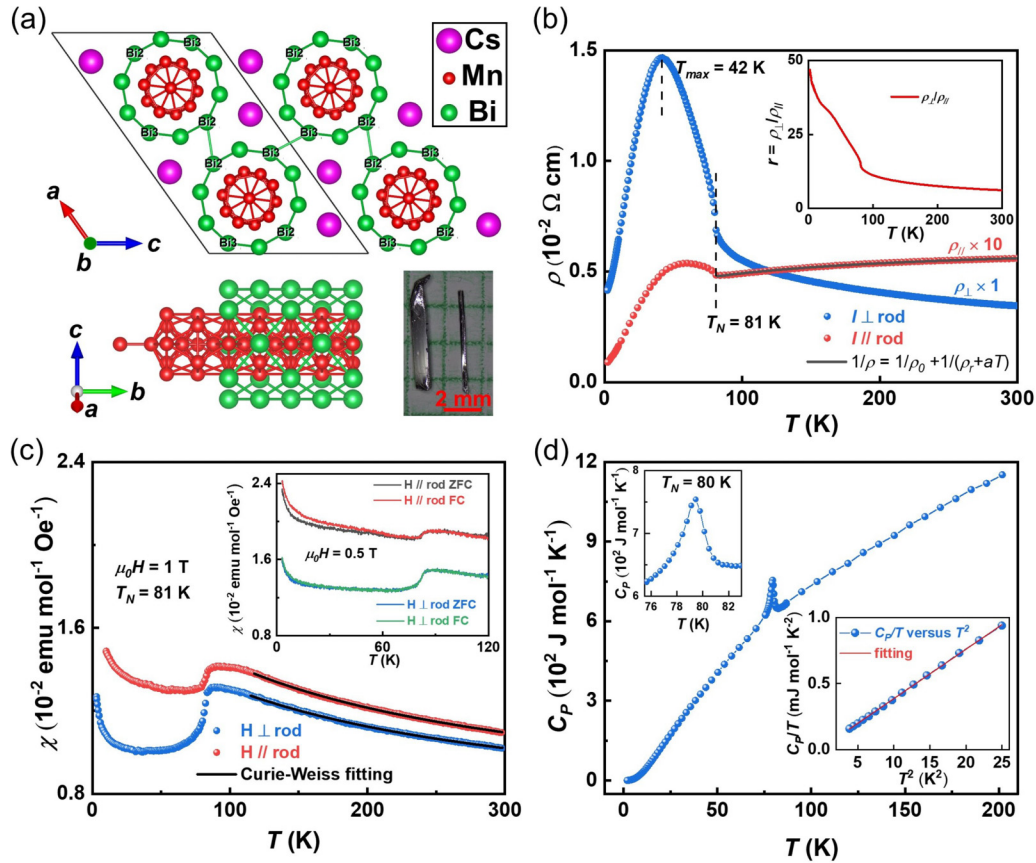


FIG. 1. Crystal structure and properties of  $\text{CsMn}_6\text{Bi}_5$  at ambient pressure. (a) Crystal structure of  $\text{CsMn}_6\text{Bi}_5$  viewed along the  $b$  axis and perpendicular to the  $bc$  plane. Intercolumn bonds  $\text{Bi}_2\text{-Bi}_2$  and  $\text{Bi}_3\text{-Bi}_3$  are labeled. Lower right shows an optical photograph of the as-grown single crystals with a grid size of 2 mm. (b) Temperature-dependent resistivity  $\rho(T)$  for  $\text{CsMn}_6\text{Bi}_5$  single crystal measured with  $I \perp \text{rod}$  and  $I \parallel \text{rod}$  ( $[010]$  direction). Black solid line is the parallel-resistor formula fit and dashed lines denote the transition temperatures. Inset shows the temperature-dependent anisotropic resistivity ratio  $r = \rho_{\perp}/\rho_{\parallel}$ . (c) Temperature-dependent magnetic susceptibility  $\chi(T)$  of  $\text{CsMn}_6\text{Bi}_5$  single crystal under 1 T for  $H \perp \text{rod}$  and  $H \parallel \text{rod}$ . Black solid lines are corresponding Curie-Weiss fittings from 110 to 300 K. Inset shows the corresponding Zero-field-cooling (ZFC) and Field-cooling (FC) curves under 0.5 T. (d) Temperature-dependent specific-heat capacity for  $\text{CsMn}_6\text{Bi}_5$  single crystal. Upper inset is the enlarged specific-heat capacity around 80 K and the lower inset shows the  $C_p/T$  vs  $T^2$ , where the red solid line is the linear fitting using the Debye model.  $T_N$  denotes the AFM ordering temperature determined by the maxima in  $d\rho/dT$ ,  $d\chi T/dT$ , and  $C_p$ .

high-pressure measurements can be found in the Supplemental Material (SM) [22,23]. It is seen that when the current is applied along the  $b$  axis, the resistance as a function of temperature displays a metallic behavior over the experimental temperature range. Upon increasing pressure to 11.6 GPa, a resistance drop is seen at 7.8 K, and a zero-resistance state is observed, as shown more clearly in Fig. 2(b). Our results indicate that pressure induces a SC transition of the  $\text{CsMn}_6\text{Bi}_5$  compound, in accordance with the results observed in  $\text{K/RbMn}_6\text{Bi}_5$  compounds [20,21]. We repeat the measurements with a new sample (sample No. 2) cut from different batches and obtain the reproducible results—increasing pressure renders the  $\text{CsMn}_6\text{Bi}_5$  compound to be SC at 12.2 GPa [Figs. 2(c) and 2(d)]. At 14.8 GPa, a zero-resistance state presents [Fig. 2(c)]. The onset SC transition temperature ( $T_c$ ) and the critical pressure ( $P_c$ ) for such a transition are similar to what has been seen in  $\text{K/RbMn}_6\text{Bi}_5$  compounds [20,21]. With further compression to 16.2 GPa, we find the sample investigated loses its zero-resistance state and  $T_c$  shifts to lower temperature. At 26 GPa, the resistance drop is not detectable

at the temperature down to 1.5 K, the lowest temperature of this study.

To further characterize the pressure-induced superconductivity, we performed the measurements for the sample No. 3 and observed the same results—the  $\text{CsMn}_6\text{Bi}_5$  compound undergoes a SC transition at 12.6 GPa [Fig. 2(f)]. Application of magnetic field at 13.3 and 17.0 GPa finds that the transition shifts to lower temperature upon increasing the field [Figs. 2(g) and Fig. S3 in the SM [22]]. We extracted the field-dependent  $T_c$  for the compressed  $\text{CsMn}_6\text{Bi}_5$  [Fig. 2(h)], and estimated the upper critical field at zero temperature by using the Ginzburg-Landau formula [24]:  $H_{c2}(T) = H_{c2}(0)[1 - (T/T_c)^2]/[1 + (T/T_c)^2]$ . The estimated values of  $H_{c2}$  are  $\sim 22.9$  T at 13.3 GPa and  $\sim 23.8$  T at 17.0 GPa, which are higher than the value of the Pauli limit ( $\mu_0 H_p = 1.84 T_c$ ) [25], implying that the pressure-induced superconductivity in  $\text{CsMn}_6\text{Bi}_5$  has an unconventional nature [25,26].

To investigate whether the pressure-induced SC transition is associated with any structural phase transition, we

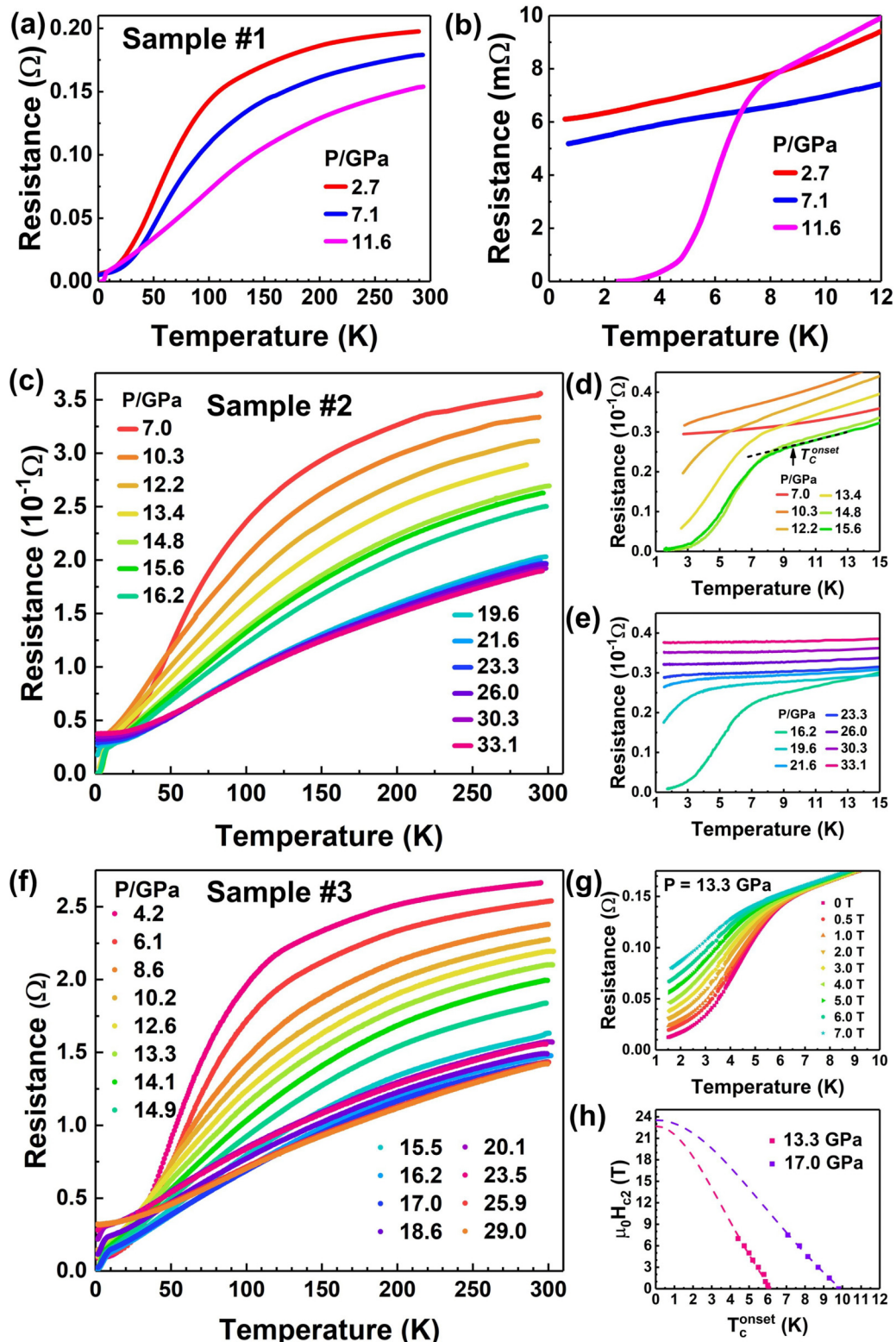


FIG. 2. Temperature dependence of the resistance and determination of upper critical field for the pressurized  $\text{CsMn}_6\text{Bi}_5$  samples. (a) Resistance results measured from 300 to 1.5 K for sample No. 1 in the pressure range of 2.7–11.6 GPa. (b) Low-temperature resistance of sample No. 1, showing a clear superconducting transition. (c) Resistance measurements on sample No. 2 in the pressure range of 7.0–33.1 GPa. (d), (e) Enlarged views of (c), displaying the details about the superconducting transition of sample No. 2. (f) Resistance results of sample No. 3 measured from 300 to 1.5 K in the pressure range of 4.2–29 GPa. (g) Resistance measurements under different magnetic fields for the pressurized sample No. 3 subjected to 13.3 GPa. (h) Plots of  $T_c$  vs upper critical field ( $H_{c2}$ ) for sample No. 3 measured at 13.3 and 17.0 GPa, respectively. Dashed lines represent the Ginzburg-Landau (GL) fits to the data of  $H_{c2}$ .

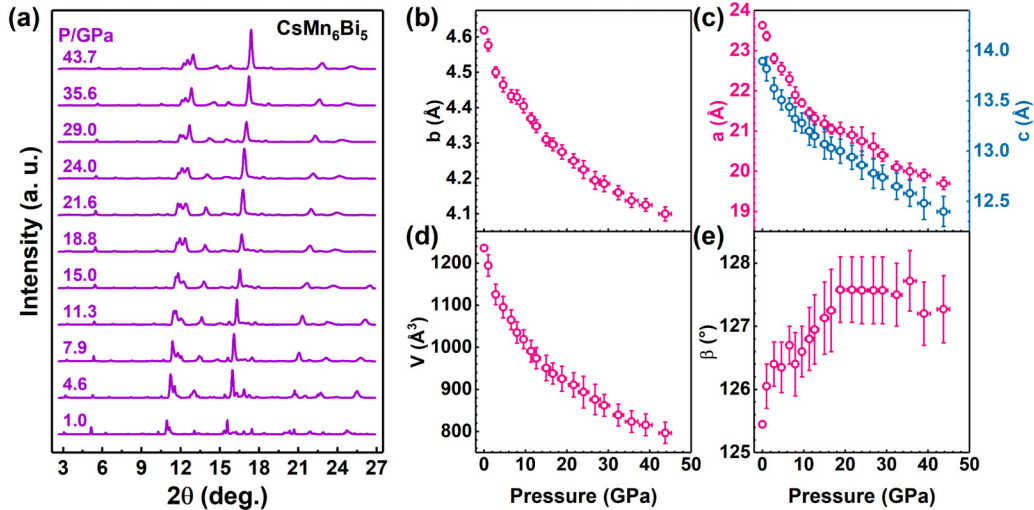


FIG. 3. X-ray-diffraction results of the CsMn<sub>6</sub>Bi<sub>5</sub> sample collected at high pressure. (a) X-ray-diffraction patterns measured at different pressures, showing no structural phase transition in the experimental pressure range up to 43.7 GPa. (b), (c) Lattice parameters  $a$ ,  $b$ , and  $c$  vs pressure. (d), (e) Pressure dependence of cell volume  $V$  and  $\beta$  angle, respectively.

performed high-pressure x-ray-diffraction (XRD) measurements on the CsMn<sub>6</sub>Bi<sub>5</sub> sample at the beamline 15W of the Shanghai Synchrotron Radiation Facility. These were high-pressure XRD measurements on the member of the AMn<sub>6</sub>Bi<sub>5</sub> ( $A = \text{K, Rb, and Cs}$ ) family. The XRD patterns collected at different pressures are shown in Fig. 3(a). For the pressures ranging from 1.0 to 43.7 GPa, within the pressure range of our transport measurements, we find that all the diffraction peaks can be indexed well by the monoclinic structure in the  $C2/m$  space group, indicating that no structural transition occurs in the pressure range. The pressure dependences of lattice parameters and cell volume are presented in Figs. 3(b)–3(d). It is seen that the lattice parameters  $a$ ,  $b$ ,  $c$ , and cell volume  $V$  decrease monotonously with increasing pressure, while the  $\beta$  angle (the angle between the  $a$  axis and the  $c$  axis) increases with pressure [Fig. 3(e)] and saturates above the pressure of 22.5 GPa.

We summarize the high-pressure transport results for the AMn<sub>6</sub>Bi<sub>5</sub> ( $A = \text{K, Rb, and Cs}$ ) family in Fig. 4(a), which includes the experimental results of AFM transition temperature ( $T_N$ ) and  $T_c$  measured from the compressed K/RbMn<sub>6</sub>Bi<sub>5</sub> [20,21]. It can be seen that application of pressure continuously suppresses  $T_N$  and suddenly induces a SC transition at the border of the AFM order state for all these compounds. Unlike other unconventional superconductors [9,27,28],  $T_N$  of these compounds terminates at a finite temperature at critical pressure, and  $T_c$  appears simultaneously at lower temperature at almost the same pressure point. This generic behavior of the family shows that the AFM state flips into a SC state at the critical pressure ( $P_c$ ). For our CsMn<sub>6</sub>Bi<sub>5</sub> samples, the measured onset  $T_c$  of the samples No. 1, No. 2, and No. 3 appears at 11.6, 12.2, and 12.6 GPa, respectively, reaches a maximum at 15.6 GPa for sample No. 2, 16.2 GPa for sample No. 3, and 14.5 GPa for sample No. 4 (Fig. S4 in the SM [22]). Upon further compression,  $T_c$ s decline monotonously and disappear at  $\sim 27$  GPa. The results of  $P(T_c)$  obtained from the measurements of CsMn<sub>6</sub>Bi<sub>5</sub> are consistent with what have been seen in K/RbMn<sub>6</sub>Bi<sub>5</sub> [20,21], suggesting that the

all-family members share the same mechanism. It is worth emphasizing that the disappearance of  $T_N$  and the appearance of  $T_c$  of AMn<sub>6</sub>Bi<sub>5</sub> ( $A = \text{K, Rb, and Cs}$ ) take place at almost the same critical pressure ( $P_c \sim 12$  GPa), and the change of  $T_c$  with pressure is also similar. Generally, the different radius of alkali metal ions  $A$  ( $A = \text{K, Rb, and Cs}$ ) should deform the lattice differently, which should result in different effects on transport behaviors, such as the different values of  $P_c$  for the AFM-SC transition and the different trends of  $P(T_c)$ . We propose that the observed similar transport results may be attributed to their unique crystal structure, because the AMn<sub>6</sub>Bi<sub>5</sub> ( $A = \text{K, Rb, and Cs}$ ) compounds have almost the same intracolumn bond lengths for the [Mn<sub>6</sub>Bi<sub>5</sub>]<sup>−</sup> columns, a kernel substructure for developing the SC state of this family (see analysis in the SM [22]).

The AFM-SC transition has been found in many compounds with 3d transition metals through chemical doping or applying pressure [4,5,7,9,29,30]. The transition can be driven by a structural phase transition [31] and quantum phase transition [4]. However, the AFM-SC transition observed in the AMn<sub>6</sub>Bi<sub>5</sub> compounds is different from what have been seen before. To understand the possible physical origin, we plot the pressure dependence of the  $\beta$  angle that represents the lattice deformation degree of the monoclinic phase in Fig. 4(b), and find that the value of  $\beta$  angle is  $\sim 125.4^\circ$  at ambient pressure, but it increases with elevating pressure, reaching  $\sim 126.8^\circ$  at  $\sim 12$  GPa where the SC state presents. This result suggests that increasing the  $\beta$  angle by  $\sim 1.4^\circ$  may be associated with the suppression of the AFM order state and the emergence of a SC state. At  $\sim 27$  GPa, a transition from a SC state to a nonsuperconducting state occurs; the  $\beta$  angle starts to show a slow decrease with pressure, implying that the  $\beta$  angle should be an effective factor in determining the electronic state of these compounds.

To further understand the correlation between the AFM and SC states for this family, we performed first-principles calculations on the electronic structure for the CsMn<sub>6</sub>Bi<sub>5</sub> sample, particularly on the partial density of states (PDOSs) of the

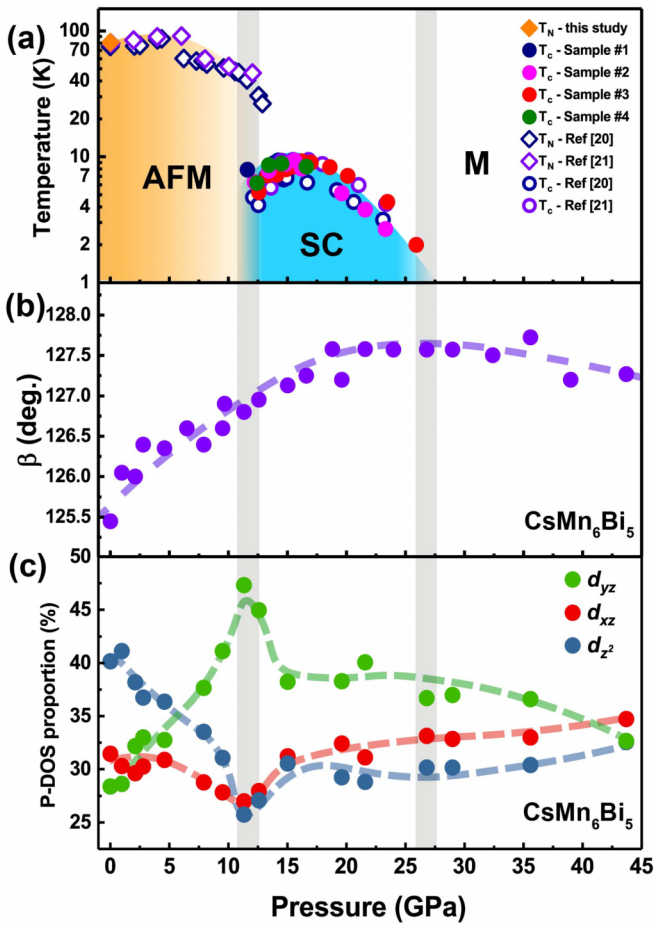


FIG. 4. Pressure-temperature phase diagram and related information for  $\text{CsMn}_6\text{Bi}_5$ . (a) Pressure-temperature phase diagram, displaying the evolution of antiferromagnetic (AFM) and superconducting (SC) states with increasing pressure. M represents the nonsuperconducting metallic state. (b) Pressure dependence of  $\beta$  angle. (c) Calculated partial density of state (PDOS) from the  $d_{yz}$ ,  $d_{xz}$ , and  $d_{z^2}$  orbital electrons of Mn atoms as a function of pressure. Dashed lines are guides for the eye.

electrons from the five  $d$  orbitals of Mn atoms, based on our high-pressure XRD results. The details about the calculations can be found in Ref. [22], and Refs. [32–35]. Since the PDOSs of the electrons from  $d_{xy}$  and  $d_{x^2-y^2}$  orbitals change continuously around the critical pressure ( $P_c = \sim 12$  GPa), where the flipping occurs, we propose that the electrons from these two orbitals have less contribution to the AFM-SC transition (see Ref. [22]). While the PDOSs of the electrons from  $d_{yz}$ ,  $d_{z^2}$ , and  $d_{xz}$  orbitals display dramatic changes at the  $P_c$ , i.e., the PDOS of the electrons from the  $d_{yz}$  orbital exhibits a peaklike behavior, but that from the  $d_{z^2}$  and  $d_{xz}$  orbitals shows a diplike behavior [Fig. 4(c)]. These results suggest that the electrons from these three orbitals may be responsible for the AFM-SC transition. The increase of the PDOS of the electrons from the  $d_{yz}$  orbital and the corresponding decrease of those from

the  $d_{z^2}$  and  $d_{xz}$  orbitals imply an orbital selective process of the Mn's  $d$  electrons around the critical pressure, which deserves further investigations.

The observed flipping of the AFM-to-SC state in this study is reminiscent of the one previously found by us in an iron-pnictide superconductor [30], where the flipping of the AFM-to-SC state occurs at a pressure-induced bicritical point. Understanding the difference and similarity of the AFM-to-SC flipping in these two families should be an attractive issue and deserves further investigations from both the experimental and theoretical sides.

### III. CONCLUSION

In summary, we report the observation of the pressure-induced superconductivity in  $\text{CsMn}_6\text{Bi}_5$  and the analysis on the generic flipping of an antiferromagnetic state to a superconducting state in the quasi-one-dimensional  $\text{AMn}_6\text{Bi}_5$  ( $A = \text{K}, \text{Rb}, \text{and Cs}$ ) compounds. We find that these three compounds show an AFM-SC transition at almost the same critical pressure ( $\sim 12$  GPa) and present the same trend in  $P(T_c)$  with almost the same superconducting dome, indicating that the different alkali metals stacked in the structure of compounds have little effect on the values of  $T_c$  and  $P_c$ . Upon further compression, the superconducting  $\text{CsMn}_6\text{Bi}_5$  converts to a nonsuperconducting metallic state at  $\sim 27$  GPa and above. Our high-pressure x-ray-diffraction measurements on the  $\text{CsMn}_6\text{Bi}_5$  sample demonstrate that no structural phase transition is found, except for a continuous decrease in lattice parameters and an increase in  $\beta$  angle. Our theoretical calculations on the  $\text{CsMn}_6\text{Bi}_5$  sample suggest that the changes of the PDOSs of the  $d_{yz}$ ,  $d_{xz}$ , and  $d_{z^2}$  orbital electrons near Fermi energy is associated with the flipping. These results may indicate that the AFM-SC transition for this family is not related to the alkali metal, but the  $[\text{Mn}_6\text{Bi}_5]$  columns, shedding insight on understanding the correlation between AFM and SC states in the unconventional SC materials dominated by the  $3d$  orbital electrons.

### ACKNOWLEDGMENTS

L. Chen, Y. Zhou, and G. Wang would like to thank Professor X. L. Chen of Institute of Physics, Chinese Academy of Sciences for helpful discussions. This work was supported by the National Key Research and Development Program of China (Grants No. 2022YFA1403900, No. 2021YFA1401800, No. 2017YFA0302902, and No. 2018YFE0202602), the National Natural Science Foundation of China (Grants No. U2032214, No. 51832010, No. 12104487, No. 12122414, and No. 12004419), and the Strategic Priority Research Program (B) of the Chinese Academy of Sciences (Grant No. XDB25000000). J.G. and S.C. are grateful for support from the Youth Innovation Promotion Association of the Chinese Academy of Sciences (Grant No. 2019008) and the China Postdoctoral Science Foundation (Grant No. E0BK111).

[1] J. G. Bednorz and K. A. Müller, Possible high  $T_c$  superconductivity in the Ba–La–Cu–O system, *Z. Phys. B: Condens. Matter* **64**, 189 (1986).

[2] M. K. Wu, J. R. Ashburn, C. J. Torng, P. H. Hor, R. L. Meng, L. Gao, Z. J. Huang, Y. Q. Wang, and C. W. Chu, Superconductivity at 93 K in a New Mixed-Phase Y-Ba-Cu-O

- Compound System at Ambient Pressure, *Phys. Rev. Lett.* **58**, 908 (1987).
- [3] Y. Kamihara, H. Hiramatsu, M. Hirano, R. Kawamura, H. Yanagi, T. Kamiya, and H. Hosono, Iron-based layered superconductor: LaOFeP, *J. Am. Chem. Soc.* **128**, 10012 (2006).
- [4] M. Rotter, M. Tegel, and D. Johrendt, Superconductivity at 38 K in the Iron Arsenide  $\text{Ba}_{1-x}\text{K}_x\text{Fe}_2\text{As}_2$ , *Phys. Rev. Lett.* **101**, 107006 (2008).
- [5] W. Wu, J. Cheng, K. Matsubayashi, P. Kong, F. Lin, C. Jin, N. Wang, Y. Uwatoko, and J. Luo, Superconductivity in the vicinity of antiferromagnetic order in CrAs, *Nat. Commun.* **5**, 5508 (2014).
- [6] D. Li, K. Lee, B. Y. Wang, M. Osada, S. Crossley, H. R. Lee, Y. Cui, Y. Hikita, and H. Y. Hwang, Superconductivity in an infinite-layer nickelate, *Nature (London)* **572**, 624 (2019).
- [7] J. G. Cheng, K. Matsubayashi, W. Wu, J. P. Sun, F. K. Lin, J. L. Luo, and Y. Uwatoko, Pressure Induced Superconductivity on the Border Of Magnetic Order in MnP, *Phys. Rev. Lett.* **114**, 117001 (2015).
- [8] T. L. Hung, C. H. Huang, L. Z. Deng, M. N. Ou, Y. Y. Chen, M. K. Wu, S. Y. Huyan, C. W. Chu, P. J. Chen, and T. K. Lee, Pressure induced superconductivity in MnSe, *Nat. Commun.* **12**, 5436 (2021).
- [9] B. Keimer, S. A. Kivelson, M. R. Norman, S. Uchida, and J. Zaanen, From quantum matter to high-temperature superconductivity in copper oxides, *Nature (London)* **518**, 179 (2015).
- [10] D. J. Scalapino, A common thread: The pairing interaction for unconventional superconductors, *Rev. Mod. Phys.* **84**, 1383 (2012).
- [11] P. Dai, J. Hu, and E. Dagotto, Magnetism and its microscopic origin in iron-based high-temperature superconductors, *Nat. Phys.* **8**, 709 (2012).
- [12] S. Sachdev and B. Keimer, Quantum criticality, *Phys. Today* **64**(2), 29 (2011).
- [13] M. R. Norman, The challenge of unconventional superconductivity, *Science* **332**, 196 (2011).
- [14] J. Paglione and R. L. Greene, High-temperature superconductivity in iron-based materials, *Nat. Phys.* **6**, 645 (2010).
- [15] N. P. Armitage, P. Fournier, and R. L. Greene, Progress and perspectives on electron-doped cuprates, *Rev. Mod. Phys.* **82**, 2421 (2010).
- [16] H. Luetkens, H. H. Klauss, M. Kraken, F. J. Litterst, T. Dellmann, R. Klingeler, C. Hess, R. Khasanov, A. Amato, C. Baines, M. Kosmala, O. J. Schumann, M. Braden, J. Hamann-Borrero, N. Leps, A. Kondrat, G. Behr, J. Werner, and B. Büchner, The electronic phase diagram of the  $\text{LaO}_{1-x}\text{F}_x\text{FeAs}$  superconductor, *Nat. Mater.* **8**, 305 (2009).
- [17] J.-K. Bao, Z.-T. Tang, H. J. Jung, J.-Y. Liu, Y. Liu, L. Li, Y.-K. Li, Z.-A. Xu, C.-M. Feng, H. Chen, D. Y. Chung, V. P. Dravid, G.-H. Cao, and M. G. Kanatzidis, Unique  $[\text{Mn}_6\text{Bi}_5]$ -nanowires in  $\text{KMn}_6\text{Bi}_5$ : A quasi-one-dimensional antiferromagnetic metal, *J. Am. Chem. Soc.* **140**, 4391 (2018).
- [18] L. Chen, L. Zhao, X. Qiu, Q. Zhang, K. Liu, Q. Lin, and G. Wang, Quasi-one-dimensional structure and possible helical antiferromagnetism of  $\text{RbMn}_6\text{Bi}_5$ , *Inorg. Chem.* **60**, 12941 (2021).
- [19] Y. Zhou, L. Chen, G. Wang, Y.-X. Wang, Z.-C. Wang, C.-C. Chai, Z.-N. Guo, J.-P. Hu, and X.-L. Chen, A new superconductor parent compound  $\text{NaMn}_6\text{Bi}_5$  with quasi-one-dimensional structure and lower antiferromagnetic-like transition temperatures, *Chin. Phys. Lett.* **39**, 047401 (2022).
- [20] Z. Y. Liu, Q. X. Dong, P. T. Yang, P. F. Shan, B. S. Wang, J. P. Sun, Z. L. Dun, Y. Uwatoko, G. F. Chen, X. L. Dong, Z. X. Zhao, and J. G. Cheng, Pressure-Induced Superconductivity up to 9 K in the Quasi-One-Dimensional  $\text{KMn}_6\text{Bi}_5$ , *Phys. Rev. Lett.* **128**, 187001 (2022).
- [21] P.-T. Yang, Q.-X. Dong, P.-F. Shan, Z.-Y. Liu, J.-P. Sun, Z.-L. Dun, Y. Uwatoko, G.-F. Chen, B.-S. Wang, and J.-G. Cheng, Emergence of superconductivity on the border of antiferromagnetic order in  $\text{RbMn}_6\text{Bi}_5$  under high pressure: A new family of Mn-based superconductors, *Chin. Phys. Lett.* **39**, 067401 (2022).
- [22] See Supplemental Material at <http://link.aps.org/supplemental/10.1103/PhysRevB.106.214515> for the experimental details, calculations and extended results.
- [23] H. K. Mao, J. Xu, and P. M. Bell, Calibration of the ruby pressure gauge to 800 kbar under quasi-hydrostatic conditions, *J. Geophys. Res.: Solid Earth* **91**, 4673 (1986).
- [24] M. Tinkham, Effect of fluxoid quantization on transitions of superconducting films, *Phys. Rev.* **129**, 2413 (1963).
- [25] A. M. Clogston, Upper Limit for the Critical Field in Hard Superconductors, *Phys. Rev. Lett.* **9**, 266 (1962).
- [26] B. S. Chandrasekhar, A note on the maximum critical field of high-field superconductors, *Appl. Phys. Lett.* **1**, 7 (1962).
- [27] G. R. Stewart, Superconductivity in iron compounds, *Rev. Mod. Phys.* **83**, 1589 (2011).
- [28] P. Gegenwart, Q. Si, and F. Steglich, Quantum criticality in heavy-fermion metals, *Nat. Phys.* **4**, 186 (2008).
- [29] P. Gao, L. Sun, N. Ni, J. Guo, Q. Wu, C. Zhang, D. Gu, K. Yang, A. Li, S. Jiang, R. J. Cava, and Z. Zhao, Pressure-induced superconductivity and its scaling with doping-induced superconductivity in the iron pnictide with skutterudite intermediary layers, *Adv. Mater.* **26**, 2346 (2014).
- [30] Y. Zhou, S. Jiang, Q. Wu, V. A. Sidorov, J. Guo, W. Yi, S. Zhang, Z. Wang, H. Wang, S. Cai, K. Yang, S. Jiang, A. Li, N. Ni, G. Zhang, L. Sun, and Z. Zhao, Observation of a bi-critical point between antiferromagnetic and superconducting phases in pressurized single crystal  $\text{Ca}_{0.73}\text{La}_{0.27}\text{FeAs}_2$ , *Sci. Bull.* **62**, 857 (2017).
- [31] Y. Kamihara, T. Watanabe, M. Hirano, and H. Hosono, Iron-based layered superconductor  $\text{La}[\text{O}_{1-x}\text{F}_x]\text{FeAs}$  ( $x = 0.05-0.12$ ) with  $T_c = 26$  K, *J. Am. Chem. Soc.* **130**, 3296 (2008).
- [32] G. Kresse and J. Hafner, *Ab initio* molecular dynamics for liquid metals, *Phys. Rev. B* **47**, 558 (1993).
- [33] G. Kresse and J. Furthmüller, Efficient iterative schemes for *ab initio* total-energy calculations using a plane-wave basis set, *Phys. Rev. B* **54**, 11169 (1996).
- [34] J. P. Perdew, K. Burke, and M. Ernzerhof, Generalized Gradient Approximation Made Simple [Phys. Rev. Lett. **77**, 3865 (1996)], *Phys. Rev. Lett.* **78**, 1396(E) (1997).
- [35] G. Kresse and J. Furthmüller, Efficiency of *ab-initio* total energy calculations for metals and semiconductors using a plane-wave basis set, *Comput. Mater. Sci.* **6**, 15 (1996).